

# Theoretical mean field and experimental occupation probabilities in the double beta decay system $^{76}\text{Ge}$ to $^{76}\text{Se}$

O. Moreno,<sup>1</sup> E. Moya de Guerra,<sup>1</sup> P. Sarriguren,<sup>2</sup> and Amand Faessler<sup>3</sup>

<sup>1</sup>*Dpto. Física Atómica, Molecular y Nuclear, Univ. Complutense de Madrid, E-28040 Madrid, Spain*

<sup>2</sup>*Instituto de Estructura de la Materia, CSIC, Serrano 123, E-28006 Madrid, Spain*

<sup>3</sup>*Institut für Theoretische Physik, Universität Tübingen, D-72076 Tübingen, Germany*

(Dated: April 13, 2022)

Usual Woods-Saxon single particle levels with BCS pairing are not able to reproduce the experimental occupation probabilities of the proton and neutron levels  $1p_{3/2}$ ,  $1p_{1/2}$ ,  $0f_{5/2}$ ,  $0g_{9/2}$  in the double-beta decay system  $^{76}\text{Ge}$  to  $^{76}\text{Se}$ . Shifting down the  $0g_{9/2}$  level by hand can explain the data but it is not satisfactory. Here it is shown that a selfconsistent Hartree-Fock+BCS approach with experimental deformations for  $^{76}\text{Ge}$  and  $^{76}\text{Se}$  may decisively improve the agreement with the recent data on occupation probabilities by Schiffer *et al.* and Kay *et al.* Best agreement with available data on  $^{76}\text{Ge}$  and  $^{76}\text{Se}$ , as well as on neighbor isotopes, is obtained when the spin-orbit strength for neutrons is allowed to be larger than that for protons. The two-neutrino double-beta decay matrix element is also shown to agree with data.

PACS numbers: 23.40.Hc, 21.60.Jz, 27.50.+e

Among double-beta decay with two neutrino processes, the best studied case is that of  $^{76}\text{Ge}$  going to  $^{76}\text{Se}$ . Within a spherically symmetric description of these nuclei, the relevant proton and neutron single particle levels involved in the double-beta decay process are in the valence shells  $1p_{3/2}$ ,  $1p_{1/2}$ ,  $0f_{5/2}$ ,  $0g_{9/2}$ . Their occupation probabilities have been recently measured by Schiffer *et al.* [1] (for neutrons) and by Kay *et al.* [2] (for protons). These data are not reproduced by previous mean field calculations using Woods-Saxon potential and pairing within BCS approximation. By increasing the binding energy of the  $0g_{9/2}$  level the agreement is better, since its occupation probability increases and eventually reaches the experimental one. This energy shifting has been performed by hand in previous works [3–5] to obtain the experimental occupation probabilities, and the resulting ground state structure has been used to compute neutrinoless double-beta matrix elements. Shell-model calculations [6] have also been carried out with occupation probabilities in good agreement with experimental ones, but the single particle energies used are not available in the literature.

In this work we use a deformed Skyrme Hartree-Fock (HF) mean field with pairing correlations within BCS approximation. At each HF iteration the BCS equations are solved to get new single particle wave functions  $\Phi_i$ , energies  $e_i$  and occupation probabilities  $v_i^2$  until convergence is achieved. After convergence, the proton-neutron quasiparticle random phase approximation (pnQRPA) equations are solved on each deformed ground state basis for  $^{76}\text{Ge}$  and  $^{76}\text{Se}$  to get their Gamow-Teller (GT) strength distributions and to compute the two-neutrino double-beta decay matrix element. The formalism is similar to that used in previous works [7–9] with an important difference. In this work we allow the Skyrme force parameters to vary and search for a parametrization that provides better agreement with the experimental occupations of the above mentioned valence shells in  $^{76}\text{Ge}$  and  $^{76}\text{Se}$ , as well as in their neighbors. We focus on the effect of the spin-orbit strength,  $W_0$ , that we find to be of primary importance for the desired description of proton and neutron valence shells occupations.

Experimental data and HF+BCS calculations suggests prolate deformations for the  $^{76}\text{Ge}$  and  $^{76}\text{Se}$  ground states. The most precise data on the quadrupole moments of these nuclei come from Coulomb excitation reorientation measurements [10] which, together with experimental charge radii [11], give a deformation parameter  $\beta = 0.10$  for  $^{76}\text{Ge}$  and  $\beta = 0.16$  for  $^{76}\text{Se}$  (with 25-30% uncertainty). These experimental deformations are taken into account when obtaining our theoretical occupation probabilities in the active shell, and naturally leads us to check if the quadrupole deformation is responsible (fully or in part) for the disagreement between previous theoretical occupations and the experimental ones. To analyze this we show in Fig. 1 the experimental occupations in the active shell together with our theoretical results for different values of the quadrupole deformation, including the experimental and selfconsistent one, constraining the quadrupole moment in the HF+BCS procedure with Sk3 Skyrme force [12]. Since the single-particle orbital and total angular momenta are not good quantum numbers in the deformed cases, a projection to a spherical basis has been performed to obtain the occupation probabilities of the spherical valence shells. The uncertainties of the experimental data, not shown in the plot, are of a few percent (less than 10%), except for the highly unoccupied  $l = 4$  proton state whose uncertainty is 30% in Se and over 100% in Ge. As the quadrupole deformation increases, the trend that can be observed in the figure is a decrease in the occupation probabilities of the states  $l = 1$  ( $1p_{3/2}$  and  $1p_{1/2}$  together) and  $l = 3$  ( $0f_{5/2}$ ) and an increase in the occupation of the state  $l = 4$  ( $0g_{9/2}$ ). Although this effect goes in the right direction, there are some features of the experimental occupations that are not reproduced by the deformed calculations as long as the deformation is constrained to reasonable values agreeing with experiment.

The most noticeable failure of the theory is a lack of occupancy in the  $0g_{9/2}$  neutron level. We have checked that this failure is shared by a large variety of the Skyrme forces where the Skyrme spin-orbit strength  $W_0$  is equal for protons and neutrons. In any case, the selfconsistent deformed single nucleon potential gives better agreement with experiment for the occupation probabilities than a Woods-Saxon potential [3, 4].

To improve agreement with experimental occupations, we found it crucial to vary the spin-orbit terms of the Skyrme energy density functional. More specifically, to increase the value of the  $W_0$  parameter in the HF+BCS potential for neutrons.

It has been already pointed out in the past that the Skyrme interactions do not reproduce properly the spin-orbit splittings of some nuclei, especially concerning neutron states, and that a more flexible two-body spin-orbit interaction is required [13]. The effect of modifying the Sk3 spin-orbit parameter  $W_0$  for neutrons is shown in Fig. 2, which contains results from a HF(Sk3 $\nu$ )+BCS calculation for spherical shape. The generalized Skyrme interaction Sk3 $\nu$  maintains the original Sk3 parametrization except for the value of the spin-orbit strength  $W_0$  for neutrons that has been replaced by a new strength  $W_\nu$  affecting only the terms of the potentials containing neutron densities. The value of the neutron strength has been modified from an initial value  $W_\nu = W_0 = 120 \text{ MeV fm}^5$  all the way up to the value  $W_\nu = 240 \text{ MeV fm}^5$ . The corresponding strength for protons has been kept fixed,  $W_\pi = W_0 = 120 \text{ MeV fm}^5$  (the units of this parameter will be omitted in the following discussions). It is worth pointing out that because of selfconsistency the change of  $W_0$  for neutrons affects not only the neutron levels but also de proton levels.

As shown in the plot, a good agreement on neutron occupation probabilities between theory and experiment is found for  $W_\nu = 200$ ; in this situation the  $0g_{9/2}$  state is more bound than the  $1p_{1/2}$  state. The result for protons yields also a good agreement with experiment; in this case, the proton state  $1p_{1/2}$  is still more bound than the state  $0g_{9/2}$ .

In Fig. 3 one can see the proton and neutron single particle energies in the active shell corresponding to the occupation probabilities of Fig. 2, together with the Fermi levels. As the spin-orbit strength for neutrons increases, the single proton and neutron levels  $1p_{1/2}$  and  $0f_{5/2}$  get clearly less bound, whereas the level  $0g_{9/2}$  gets more bound. The level  $0g_{9/2}$  exchanges its energy position with the level  $1p_{1/2}$  in the vicinity of  $W_\nu = 240$  in the case of protons and for  $160 < W_\nu < 200$  in the case of neutrons. In this last case, the level  $0g_{9/2}$  also exchanges its energy position with the level  $0f_{5/2}$  but in the range  $200 < W_\nu < 240$ . Finally, the level  $1p_{3/2}$ , which is in general the most bound of them, remains with about the same binding energy. In what follows we refer to the interaction with  $W_\pi = 120$  and  $W_\nu = 200$  as Sk3 $\nu$ .

The considerable improvement obtained by setting different values of the spin-orbit interaction for each type of nucleon supports a modification of the spin-orbit term in the general Skyrme interaction [14], that could have a structure similar to that of the other Skyrme terms, namely containing a factor of the form  $(1 + \epsilon P_\tau)$ , where  $P_\tau$  is an isospin-exchange operator. More involved isospin-dependent formulations are also possible and worth exploring.

We show in Fig. 4 the occupation probabilities in the active shells obtained with spherical HF(Sk3)+BCS and with the improved HF(Sk3 $\nu$ )+BCS (using  $W_\pi = 120$  and  $W_\nu = 200$ ) and the experimental deformation. The results are also compared to the experimental data. All of them are normalized so that the total number of nucleons in the active shells is the expected one: 4 protons and 16 neutrons in  $^{76}\text{Ge}$  and 6 protons and 14 neutrons in  $^{76}\text{Se}$ . In our calculations the actual numbers of protons and neutrons in these valence shells are lower, especially in the deformed cases, where the occupation probabilities are spread along many spherical single particle states, not only in those active shells of the spherical shell model. When obtaining the occupations from experiment, a similar (although not identical) renormalization procedure was also performed (see [1, 2] for details). As seen in the figure, the improvement reached by combining the effect of deformation and modified spin-orbit strength with respect to the spherical HF(Sk3 $\nu$ )+BCS is apparent. It is possible however that other ingredients are still missing which could enhance the trend initiated by deformation and spin-orbit strength towards a reliable description of the single particle spectrum in this nuclear region.

This new spin-orbit strength can be applied to the neighbor nuclei  $^{74}\text{Ge}$  and  $^{78}\text{Se}$ , whose active-shell occupation probabilities have been also measured [1, 2]. In Fig. 5 we compare the measured probabilities with our theoretical results for the HF(Sk3)+BCS calculation with spherical shape and for the new HF(Sk3 $\nu$ )+BCS calculation with experimental deformations. The  $\beta$ -values extracted from data in refs. [10, 11] are  $\beta = 0.13$  for  $^{74}\text{Ge}$  and  $\beta = 0.12$  for  $^{78}\text{Se}$ . The inclusion of experimental deformation and a larger spin-orbit strength for neutrons change also in this case the theoretical results towards a better agreement with the experimental data.

The new single particle energies and occupation probabilities have also an effect on the matrix element of the two-neutrino double-beta decay  $^{76}\text{Ge} \rightarrow ^{76}\text{Se}$ . In Fig. 6 we show the theoretical double-beta decay matrix element running sum as a function of the excitation energy of the intermediate nucleus  $^{76}\text{As}$ . The results shown correspond to deformed pnQRPA calculations (see ref. [8] and references therein for details of calculations) using the single particle basis for  $^{76}\text{Ge}$  and for  $^{76}\text{Se}$  obtained with the new (Sk3 $\nu$ ,  $W_\nu > W_\pi$ ) and the standard (Sk3,  $W_\nu = W_\pi = W_0$ ) parametrizations, with and without deformation. Proton-neutron particle-hole  $ph$  and particle-particle  $pp$  residual interactions within QRPA are included to obtain the contributions to the double-beta matrix element, following the procedure explained in previous works [8]. The coupling constants of the  $ph$  and  $pp$  channels take the values  $\chi_{ph} =$

0.25 MeV and  $\kappa_{pp} = 0.08$  MeV respectively. In the case of  $\chi_{ph}$ , it is an average value between the one used in previous works [9, 15, 16] and the selfconsistent value [17]. In the case of  $\kappa_{pp}$ , the current value is in agreement with the one used in some previous works [8, 16], but it is twice as large as the one in [9]. We note that the larger value of the  $pp$  residual interaction coupling constant is responsible for the particular shape of the plots in Fig. 6, where the matrix element increases in the region from 0 to 4 MeV of excitation energy, then goes up and down with increasing energy and finally decreases until reaching its final value. This behavior does not show up for the smaller values of the  $pp$  coupling constant in [9]. This finding also agrees with the conclusions reached in ref. [18], namely that the characteristic increase and decrease with energy of the matrix element found in many shell model calculations is also found in our deformed pnQRPA calculations when we use larger values of  $\kappa_{pp}$  than those used in our previous works [9].

The experimental data shown in Fig. 6 are obtained in a phenomenological way using the experimental Gamow-Teller (GT) strengths of the transitions  $^{76}\text{Ge} \rightarrow ^{76}\text{As}$  (GT<sup>-</sup>) [19] and  $^{76}\text{Se} \rightarrow ^{76}\text{As}$  (GT<sup>+</sup>) [20], as explained in previous experimental or theoretical works [9, 20]. An experimental range for the final value of the matrix element is also shown in the plot, obtained from the experimental double-beta decay half-life [21] with two possible values of the axial-to-vector ratio  $g_A = 1.25$  and  $g_A = 1.00$  (quenched value).

It is clearly seen in the figure that the calculations with the increased spin-orbit strength for neutrons reproduce much better the experimental values. In the low energy region the agreement is improved with deformation. There are no large differences between the calculations with spherical ground states and the one with experimental deformations. For Sk3' both of them lie within the experimental range for the total value of the matrix element. For Sk3 a large disagreement is found with the  $\kappa_{pp}$  value used here.

We can trace back the origin of the low-energy behavior of the double-beta matrix element, studying the accumulated strength distributions of the GT<sup>-</sup> transition  $^{76}\text{Ge} \rightarrow ^{76}\text{As}$  and of the GT<sup>+</sup> transition  $^{76}\text{Se} \rightarrow ^{76}\text{As}$ . In the case of the GT<sup>-</sup> strength distribution, our result with  $W_\nu > W_\pi$  is roughly twice as large as the result with the usual strength ( $W_\nu = W_\pi = W_0$ ) until 4 MeV, and the former reproduces better the experimental data in this range. In the case of the GT<sup>+</sup> strength distribution, the results with increased spin-orbit strength are again larger, and there is a big difference between the spherical or the deformed single particle basis for  $^{76}\text{Se}$ . The deformed one gives the best agreement with the results using experimental data. Beyond 2 MeV the experimental value increases, whereas the theoretical results wait until 5 MeV to do so (not shown in the plot).

From this analysis we conclude that the better agreement between theoretical and experimental occupation probabilities in the valence states with deformation and enhanced neutron spin-orbit gives rise to GT transitions in good agreement with the experimentally known strengths at low energy that involve the valence shells. This in turn produce a better agreement for the double-beta matrix element.

Apart from the single- and double-beta decay properties of the nuclei under study, the modification of the neutron spin-orbit strength affects some bulk properties of the nuclei, in particular the binding energy and the charge radius. Since the parameters of the Skyrme interactions are fitted to reproduce these bulk properties in a given set of nuclei, the modification of one of them without an overall refitting of the rest may result in unrealistic values of those bulk properties. Notwithstanding the above, when comparing with the experimental binding energies of 661.6 MeV for  $^{76}\text{Ge}$  and 662.07 MeV for  $^{76}\text{Se}$  we get a 0.5% underestimation in the calculation with the usual Sk3 force and a 2% overestimation in the calculation with the Sk3' force. Concerning the charge radii, the HF(Sk3)+BCS results are 4.12 fm for  $^{76}\text{Ge}$  and 4.17 fm for  $^{76}\text{Se}$ , whereas with increased spin-orbit strength one gets 4.09 fm for  $^{76}\text{Ge}$  and 4.14 fm for  $^{76}\text{Se}$ , which actually agree better with the experimental values of 4.08 fm for  $^{76}\text{Ge}$  and of 4.14 fm for  $^{76}\text{Se}$  [11].

To conclude, we have shown that agreement with experimental occupation numbers in the valence shells of  $^{76}\text{Ge}$  and  $^{76}\text{Se}$  can be obtained within the selfconsistent Skyrme+HF+BCS deformed mean field approximation. Best agreement with experiment is obtained when a spin-orbit interaction more flexible than the standard one in Skyrme forces is considered, allowing in particular for a larger neutron spin-orbit force. We point out that the interplay between spin-orbit strengths and deformation is an essential feature to give the experimental occupations. These occupation numbers are in turn of great importance for beta strength distributions and two-neutrino double-beta decay matrix element calculations, especially in the low energy region. Changes at the level of the two-body Skyrme interaction and energy density functional are suggested to further improve the theoretical description of nuclei and will be further investigated.

We acknowledge the support of the Internationales Graduiertenkolleg GRK683 of the DFG and the Sonderforschungsbereich TR27, Ministerio de Ciencia e Innovación (Spain) under Contract. Nos. FIS2008-01301 and CSPD-2007-00042@Ingenio2010; and CSIC-UCM 'Grupo de Física Nuclear' - 910059 and FPA-2007-62616.

---

[1] J.P. Schiffer *et al.*, Phys. Rev. Lett. **100**, 112501 (2008).

- [2] B.P. Kay *et al.*, Phys. Rev. C **79**, 021301(R) (2009).
- [3] J. Suhonen, O. Civitarese, Phys. Lett. B **668**, 277 (2008).
- [4] F. Simkovic, A. Faessler, P. Vogel, Phys. Rev. C **79**, 015502 (2009).
- [5] J. Barea, F. Iachello, Phys. Rev. C **79**, 044301 (2009).
- [6] J. Menéndez, A. Poves, E. Caurier, F. Nowacki, Phys. Rev. C **80**, 048501 (2009).
- [7] P. Sarriguren, E. Moya de Guerra, L. Paceaescu, A. Faessler, F. Simkovic, A.A. Raduta, Phys. Rev. C **67**, 044313 (2003).
- [8] R. Álvarez-Rodríguez, P. Sarriguren, E. Moya de Guerra, L. Paceaescu, A. Faessler, F. Simkovic, Phys. Rev. C **70**, 064309 (2004).
- [9] O. Moreno, R. Álvarez-Rodríguez, P. Sarriguren, E. Moya de Guerra, F. Simkovic, A. Faessler, J. Phys. G: Nucl. Part. Phys. **36**, 015106 (2009).
- [10] P. Raghavan, Atomic and Nuclear Data Tables **42**, 189 (1989); N.J. Stone, Table of Nuclear Moments (2001), [www.nndc.bnl.gov/nndc/stone\\_moments](http://www.nndc.bnl.gov/nndc/stone_moments)
- [11] I. Angeli *et al.*, Atomic Data and Nuclear Data Tables **87**, 185 (2004).
- [12] M. Beiner, H. Flocard, N. Van Giai, P. Quentin, Nucl. Phys. A **238**, 29 (1975).
- [13] P.-G. Reinhard, H. Flocard, Nucl. Phys. A **584**, 467 (1995); G.A. Lalazissis, D. Vretenar, W. Pöschl, P. Ring, Phys. Lett. B **418**, 7 (1998); E. Chabanat, P. Bonche, P. Haensel, J. Meyer, R. Schaeffer, Nucl. Phys. A **635**, 231 (1998).
- [14] D. Vautherin and D.M. Brink, Phys. Rev. C **5**, 626 (1972).
- [15] H. Homma, E. Bender, M. Hirsch, K. Muto, H.V. Klapdor-Kleingrothaus, T. Oda, Phys. Rev. C **54**, 2972 (1996).
- [16] M. Saleh, V. Rodin, A. Faessler, F. Simkovic, Phys. Rev. C **79**, 014314 (2009).
- [17] P. Sarriguren, E. Moya de Guerra, A. Escuderos, A. Carrizo, Nucl. Phys. A **635**, 55 (1998).
- [18] D. Fang, A. Faessler, V. Rodin, M. Saleh, F. Simkovic, arXiv:0910.3090.
- [19] R. Madey *et al.*, Phys. Rev. C **40**, 540 (1989).
- [20] E.-W. Grewe *et al.*, Phys. Rev. C **78**, 044301 (2008).
- [21] A. Barabash, arXiv:nucl-ex/0602009v2 (2006).

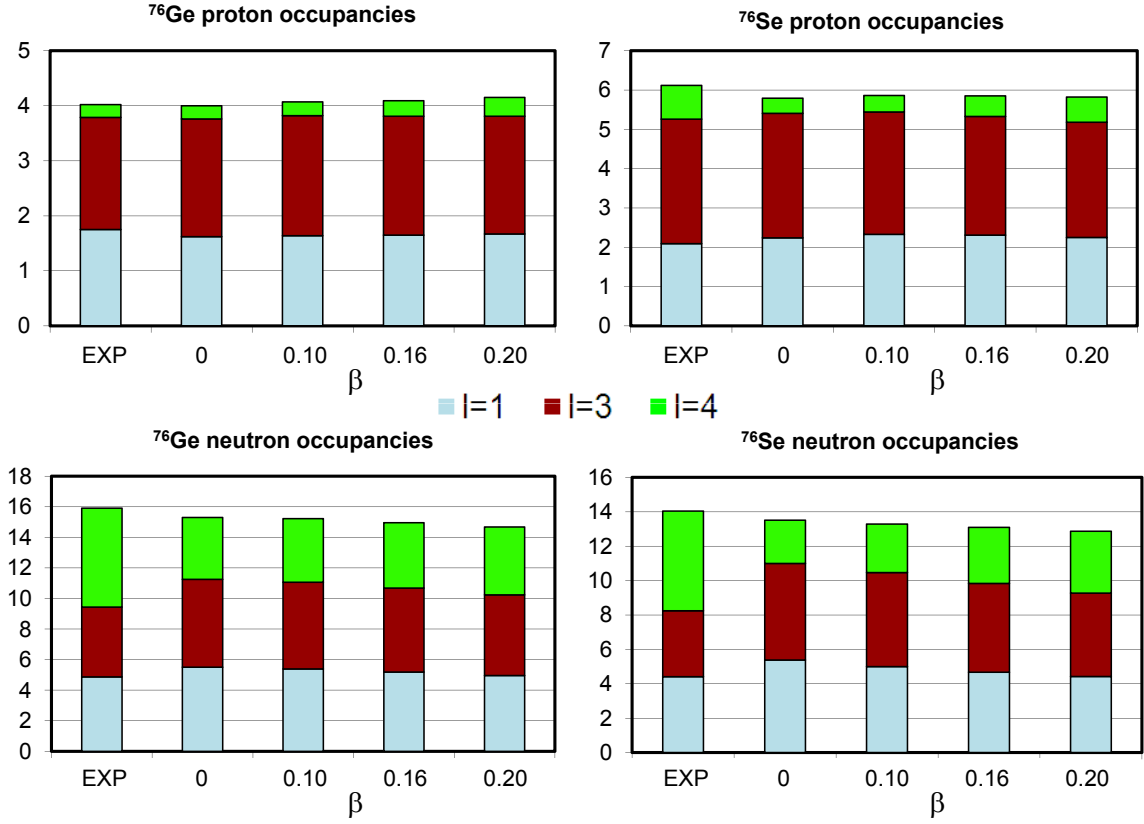


FIG. 1: (Color online) Active-shell experimental [1, 2] and theoretical occupations for different quadrupole deformations (indicated by the deformation parameter  $\beta$ ), from a HF(Sk3)+BCS calculation in  $^{76}\text{Ge}$  and  $^{76}\text{Se}$ . Occupations are shown for the proton and neutron states in the active shells, which include the single particle states  $1p_{1/2}$  and  $1p_{3/2}$  (gathered as  $l = 1$ ),  $0f_{5/2}$  ( $l = 3$ ) and  $0g_{9/2}$  ( $l = 4$ ).

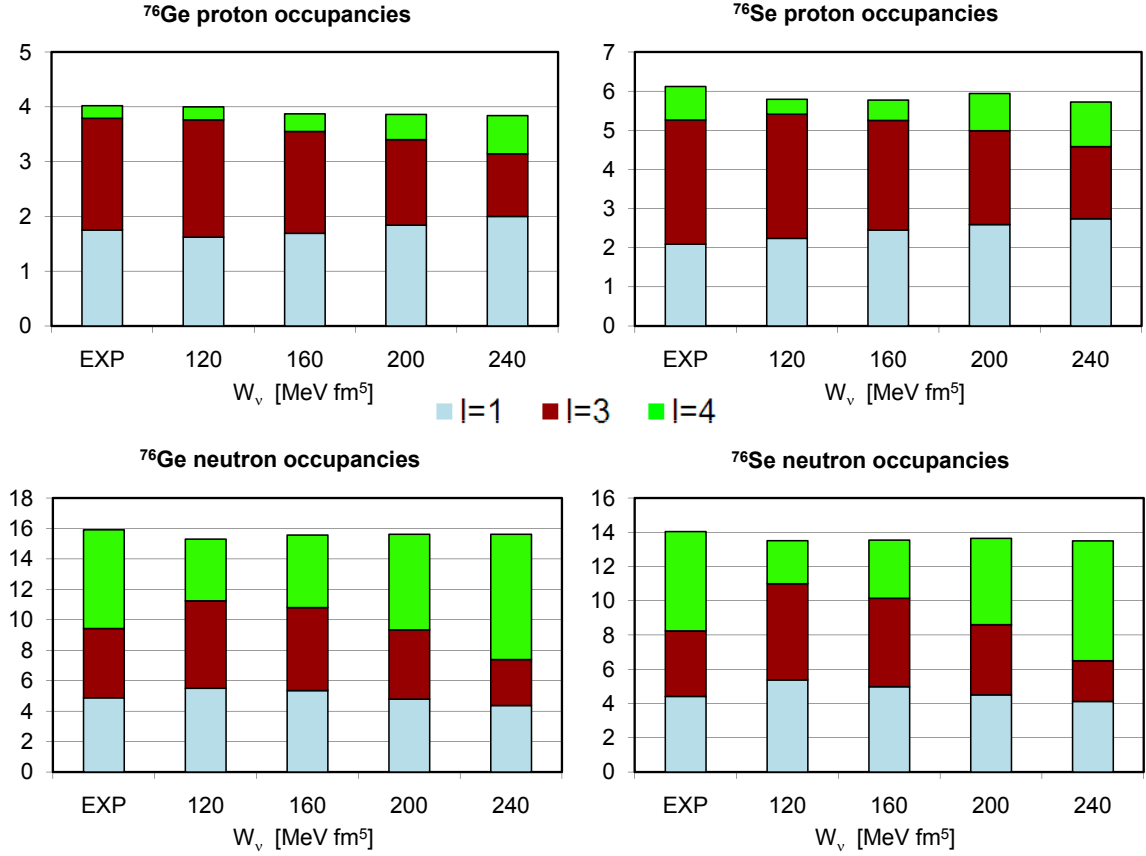


FIG. 2: (Color online) Active-shell experimental [1, 2] and theoretical occupancies for different values of the neutron spin-orbit strength  $W_\nu$  (with  $W_\pi = 120$ ), from a HF(Sk3 $\nu$ )+BCS calculation in  $^{76}\text{Ge}$  and  $^{76}\text{Se}$  with spherical ground states.

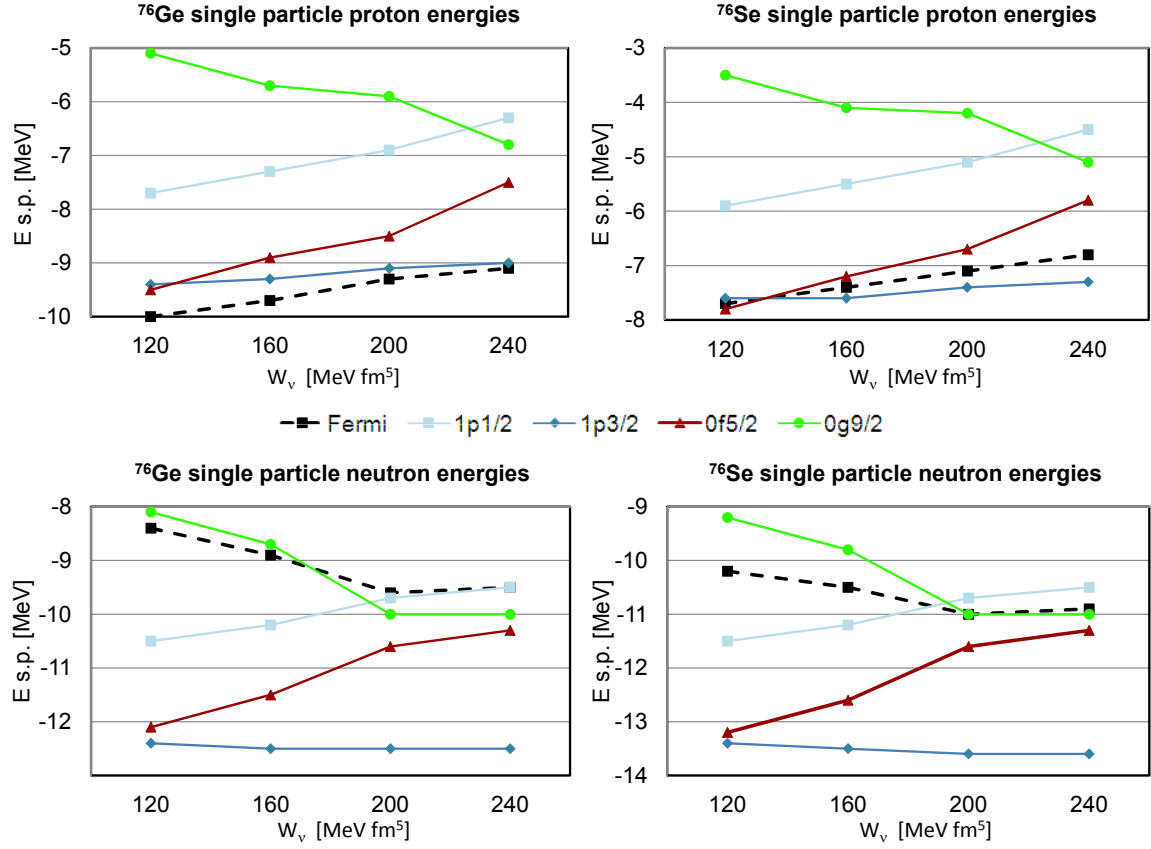


FIG. 3: (Color online) Theoretical Fermi levels and active-shell single particle energies for different values of the neutron spin-orbit strength  $W_\nu$  (with  $W_\pi = 120$ ), from a HF(Sk3')+BCS calculation in  $^{76}\text{Ge}$  and  $^{76}\text{Se}$  with spherical ground states. The occupations corresponding to these levels appeared in Fig. 2.

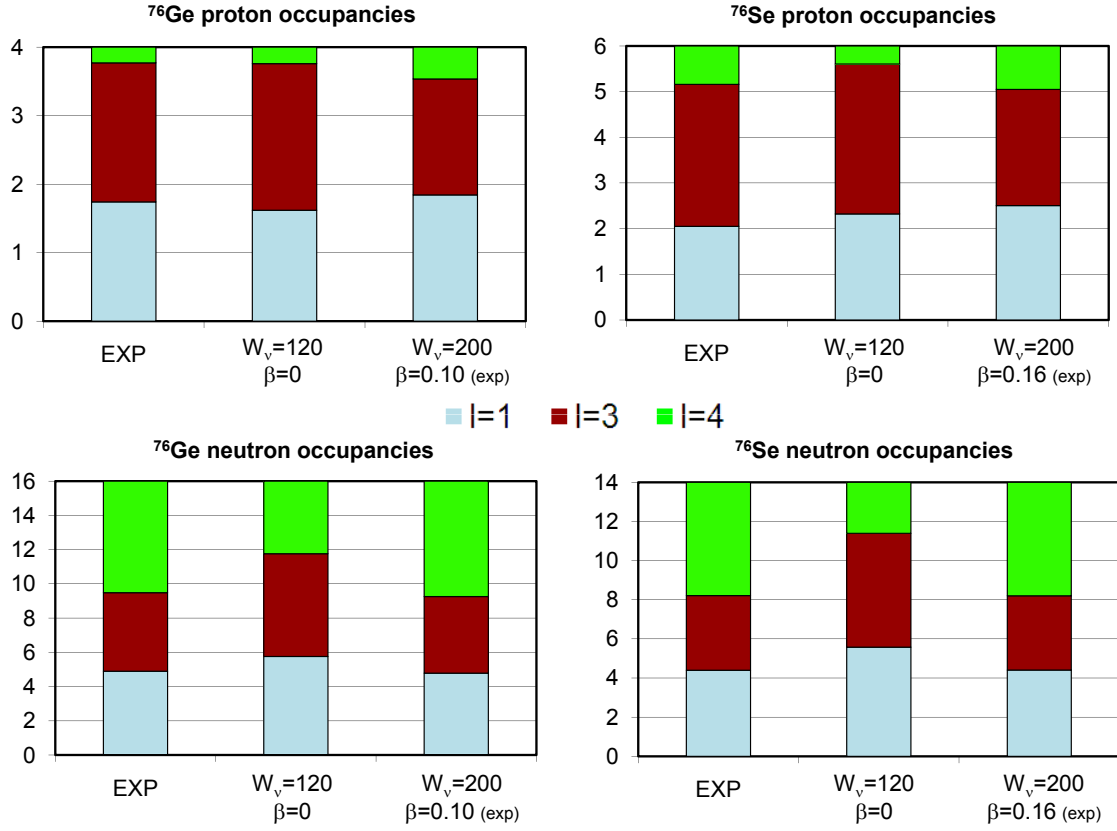


FIG. 4: (Color online) Active-shell experimental [1, 2] and theoretical occupancies in  $^{76}\text{Ge}$  and  $^{76}\text{Se}$ . The first theoretical result is the original HF(Sk3)+BCS calculation for spherical ground states and the second one is the HF(Sk3') + BCS calculation with  $W_\nu = 200$  and experimental ground-state deformations [10]. Both experiment and theory have been normalized so that the active shell contains all the nucleons exceeding the magic number 28.



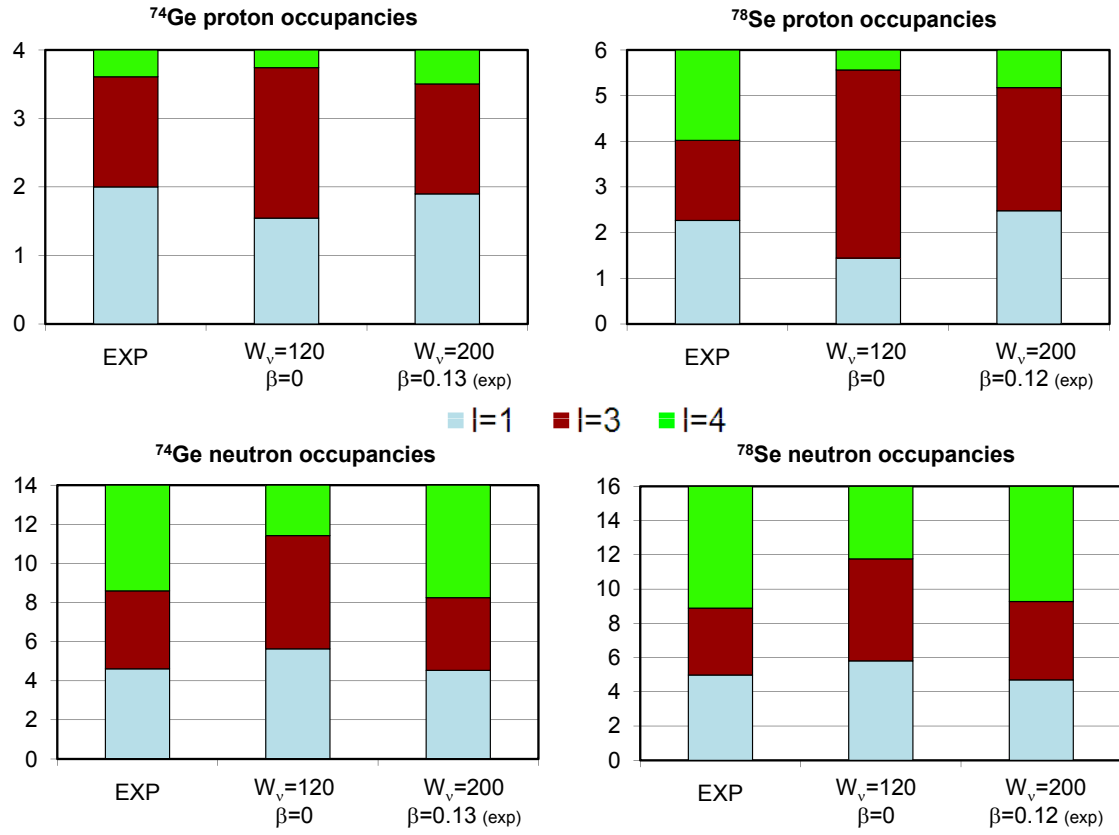


FIG. 5: (Color online) Same as in Fig. 4 but for <sup>74</sup>Ge and <sup>78</sup>Se.

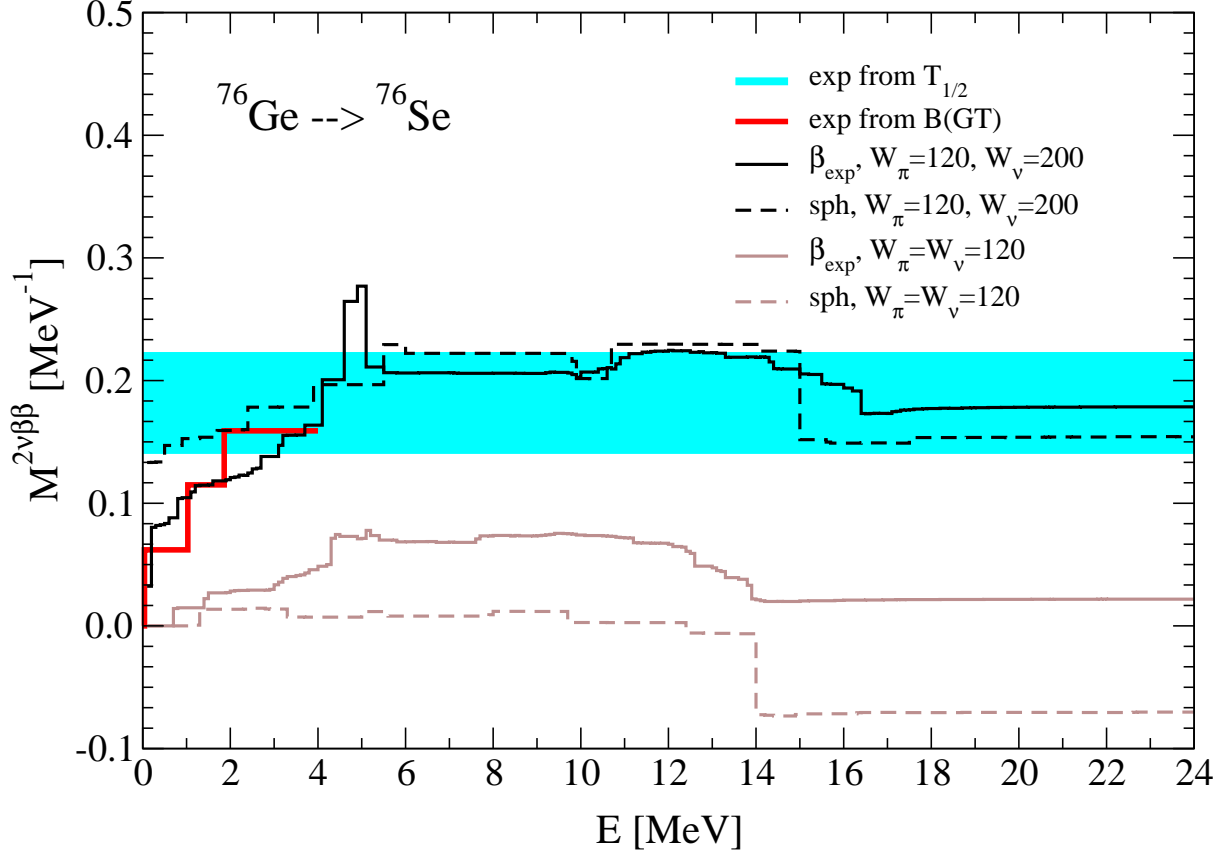


FIG. 6: (Color online) Running sum of the matrix element for the two-neutrino double-beta decay  $^{76}\text{Ge} \rightarrow ^{76}\text{Se}$ , as a function of the intermediate excitation energy in  $^{76}\text{As}$ . The single particle basis for  $^{76}\text{Ge}$  and  $^{76}\text{Se}$  have been obtained from HF(Sk3 $\nu$ )+BCS ( $W_{\nu} > W_{\pi}$ ) and from HF(Sk3)+BCS ( $W_{\nu} = W_{\pi} = W_0$ ) calculations for spherical (sph) and experimental deformed (exp def) ground state shapes. An experimental range of the total matrix element is shown, coming from the experimental half-life of the process. The experimental low-energy steps of the matrix element running sum come from experimental GT $^+$  and GT $^-$  strengths [20].